Nanoscale

Velcro-Mimicking Surface Based on Polymer Loop Brushes

Journal:	*Nanoscale*
Manuscript ID	NR-ART-07-2018-005526.R1
Article Type:	Paper
Date Submitted by the Author:	09-Sep-2018
Complete List of Authors:	Zhou, Tian; Drexel University, Materials Science and Engineering Han, Biao; Drexel University, School of Biomedical Eng, Sci and Health Systems Qi, Hao; Drexel University, Materials Science and Engineering Pan, Qiwei; Drexel Univ, MSE Smith, Derrick; Drexel University, Materials Science and Engineering Han, Lin; Drexel University, School of Biomed. Eng. Sci. & Health Syst. li, christopher; Drexel University, Materials Science and Engineering

Journal Name

ARTICLE

Velcro-Mimicking Surface Based on Polymer Loop Brushes

Received 00th January 20xx,
Accepted 00th January 20xx

DOI: 10.1039/x0xx00000x

www.rsc.org/

Tian Zhou,[a] Biao Han,[b] Hao Qi,[a] Qiwei Pan,[a] Derrick M. Smith,[a] Lin Han,[b] and Christopher Y. Li *[a]

We herein report the fabrication of Velcro-mimicking surface based on polymer brushes. Using Poly(ε-caprolactone) (PCL) as the model polymer, polymer loop brushes (PLBs) and singly tethered polymer brushes (STPBs) with nearly identical tethering point density and brush heights were synthesized using a polymer single crystal (PSC)-assisted grafting-to method. Atomic force microscopy-based single molecular force spectroscopy (AFM-SMFS) and macroscale lap-shear experiments both demonstrated that the PLBs led to strong adhesion that is up to ~ 10 times greater than the STPBs, which is attributed to the enriched chain entanglement between the probing polymer and the brushes. We envisage that our results pave the way towards a new materials design for strong adhesives and naocomposites.

1. Introduction

Miniaturization of Velcro-like (loop/hook) interaction has been found in many biological processes requiring strong adhesion including cell aggregation, antigen recognition and mitosis.[1-3] To mimic this behaviour, several approaches based on supramolecular recognition have been proposed and the resultant materials outperform some commercial adhesives.[4, 5] In polymeric systems, the construction of molecular Velcro structures is frequently observed through entanglement of polymer loops with free chain ends at polymer/polymer interfaces.[6] To apply the polymer entanglement concept in the design and fabrication of the Velcro-inspired adhesives, well-defined polymer loop brushes (PLBs) are needed. There have been a number of reports on synthesizing PLBs by adsorption of telechilic/triblock copolymers,[7-9] yet the majority of the studies have been focusing on reducing bio-adhesion by replacing singly tethered polymer brushes (STPBs) with PLBs,[10, 11] mostly due to that a more rigid loop chain conformation and slower chain dynamics of PLBs compared with STPBs.[12-16] Thus, mimicking "molecular Velcro" with PLBs could pave the way towards the construction of highly robust adhesives.

We recently developed a new strategy to synthesize well-defined polymer brushes by using a polymer single crystal (PSC)-assisted grafting-to method.[17] Herein we report the fabrication of molecular Velcro-mimics using precisely synthesized PLBs. Both PLBs and STPBs with nearly identical structure (e.g. grafting density, chain blob density) have been investigated. The molecular weight of both polymer brushes was kept to be lower than the critical polymer entanglement molecular weight (M_c) to investigate the loop effect.[18, 19] Atomic force microscopy-based single molecular force spectroscopy (AFM-SMFS) was utilized to investigate the interaction between free chain end and the polymer brush surface. Statistical analysis of the force spectra showed significantly enhanced adhesion between the polymer-bearing AFM force probe and PLBs as compared with STPBs. At macroscale, lap shear adhesion tests demonstrated that when a glass surface is modified with PLBs, 10 times stronger adhesion can be obtained compared with those modified with STPBs.

2. Experimental

Materials

ε-caprolactone (CL) was purchased from Aldrich and distilled under reduced pressure before use. Hydroxyl-terminated Poly(ε-caprolactone) (M_w ~ 38 kDa, degree of polymerization (DP) ~ 333, PDI = 1.5) (PCL_{333}-OH) was purchased from Polymer Source, Inc. (5-methoxy-1,3-phenylene)dimethanol, (4-methoxyphenyl)methanol, tin(II) 2-ethylhexanoate, 3-(triethoxysilyl)propyl isocyanate, dibutyltin dilaurate and 2-aminoethanol hydrochloride were purchased from Aldrich and used without further purification. 1-butanol was purchased from Aldrich and was distilled to remove impurities before use. All other chemicals were purchased from Aldrich and used as received.

Characterizations

^{1}H nuclear magnetic resonance (NMR) spectra were recorded on a Varian 500 MHz spectrometer using $CDCl_3$ as the solvent and tetramethylsilane (TMS) as the internal standard. Gel permeation chromatography (GPC) tests were carried out using a Waters GPC with 1525 binary HPLC pump and a Waters

[a] Department of Materials Science and Engineering, Drexel University, Philadelphia, PA 19104, United States. Email: chrisli@drexel.edu.
[b] School of Biomedical Engineering, Science and Health Systems, Drexel University, Philadelphia, PA 19104, United States.
Electronic Supplementary Information (ESI) available: Detailed experimental procedures. See DOI: 10.1039/x0xx00000x

2414 refractive index detector. All GPC samples were conducted using tetrahydrofuran as the carrier solvent with a flow rate of 1.0 mL/min at 30 ^{o}C. Standard monodispersed polystyrenes (Shodex standard, Kawasaki, Japan) were used for calibration. Atomic force microscopy (AFM) imaging experiments were conducted on a Bruker Dimension Icon system. Tapping mode was used for imaging of PSCs, PLBs and STPBs in air. Specifically, TESPA silicon probes (Bruker, Camarillo, CA) with spring constant k ~ 42 N/m and resonance frequency ~ 320 kHz were used, and the images were acquired with 512 × 512 points at a scan rate of ~ 1.0 Hz per line. PeakForce QNM mode in liquid was used for the imaging of polymer brushes in toluene. In these experiments, Si_3N_4 probes (k ~ 0.27 N/m) (BudgetSensors, Sofia, Bulgaria) were used with Bruker fluid cell (DECAFMCH-PFT). Before each experiment, the reflection sensitivity and spring constant of the cantilever were calibrated using thermal fluctuation method. The PeakForce setpoint was set to 500 pN where negligible deformation of the brush samples occurred. Images were then acquired with 256 × 256 points at a scan rate of ~ 1.0 Hz per line.

AFM-SMFS tests were carried out on both PLBs and STPBs at room temperature using a Dimension Icon AFM (Bruker Nano, Santa Barbara, CA) and a polymer chain grafted Si_3N_4 AFM probes. For each tip and sample (PLBs or STPBs) combination, at least 10 locations were picked up randomly and tested to give over 800 force curves. At each location, the probe tip was programmed to approach to, indent and then retract from the sample at a 500 nm/s constant z-piezo displacement rate (approximately equals the indentation depth rate) up to a ~2 nN maximum indentation force. Before retraction, a surface delay time (t_d=0 or 10 s) was applied to allow further interaction between AFM probe and brush samples. For each curve from a location, the cantilever deflection (in volts) and z-piezo displacement (in µm) were converted to an indentation force (in nN) and distance (in nm) through calibrating the cantilever deflection sensitivity (nm/V) by indenting on a hard mica substrate and a spring constant (nN/nm) via thermal vibration. For data analysis, the approaching portion of the force-distance curves obtained from the AFM-SMFS were firstly baseline corrected. Distance was set to 0 at maximum force for each curve. Representative curves were plotted to illustrate the repulsion from polymer brush layers (see Supporting Information). The unloading portion of the curves at each location were also noise filtered and baseline corrected. Then the curves were hand-picked to identify the existence of adhesion force. For each curve, the effective contact point of the curve was determined as the last point with force larger than 3 times the standard deviation of the flat part of the curve. Then the maximum adhesion force was determined as the absolute value of the adhesion force from the retract curve. The corresponding distance was determined as the distance between the minimum force point and the effective contact point.

Shear adhesion tests to evaluate the adhesive properties of polymer brush coated glass substrates were performed using a house-made apparatus as illustrated in Scheme S2. Three series of parallel experiments using bare glass, STPBs grafted glass and PLBs grafted glass were conducted. The STPBs grafted and PLBs grafted glass substrates were prepared by dropcasting PSCs suspension in 1-butanol onto clean glass slides followed by immobilization and washing. This approach ensures nearly 100% surface coverage. To prepare a pair of samples, a PCL film (MW ~ 80 kDa) with thickness around 200 µm was sandwiched between two glass slides with identical functional surface coating. The glass slides were press together on a hot stage at 80 ^{o}C using a 500 g weight for 30 min or overnight. The shear adhesion measurements were performed at room temperature, and the adhesion strength for each substrate-PCL film combination was calculated by dividing the load (N) corresponding to the breaking points by adhesion area (m^2). To understand the failure mechanism of each sample combination, scanning electron microscopy (SEM) imaging was used to examine the fracture surfaces.

3. Results and discussions

PSCs are typically quasi-two dimensional (2D) in nature with a thickness of ~ 10 nm while the lateral dimensions can be a few hundred micrometers and they have been recently used in numerous applications.[20-29] In a 2D PSC, polymer chains fold back and forth in the crystal as shown in Figure 1a, where *l* is the thickness of the crystal, *d* is the average distance between the adjacent chains. When the polymer chains are controlled to fold integral times (fold number n = 1, 2, etc.), the end functional groups would reside on the surface of the crystal and they can be used for subsequent chemical coupling.[17] In this study, two polymers were specifically chosen: monofunctionalized PCL_{28}-$Si(OC_2H_5)_3$ and telechelic $(H_5C_2O)_3Si$-PCL_{56}-$Si(OC_2H_5)_3$, where 28 and 56 denote DP of the two polymers, respectively (See Supporting Information, Figures S1, S2). Controlled PSCs were formed using self-seeding (Scheme S1) and the alkoxysilane groups were excluded onto the PSC surface. Upon chemically coupling the PSCs to a glass substrate catalyzed with ammonia vapor and washing away excessive polymers, polymer brushes with controlled architecture can be obtained as shown in Figures 1a, b, where σ is the grafting density, ε describes the average adjacent chain distance, ε' is the average chain end-to-end distance of a loop, and *h* is the brush layer height. Note that when a telechelic $(H_5C_2O)_3Si$-PCL_{56}-$Si(OC_2H_5)_3$ is used and when such a polymer chain folds *odd*-number times in the crystal, both chain ends are exposed onto the *same* side of lamellar surfaces as illustrated in Figure 1a. Coupling chain ends to the solid substrate leads to doubly tethered polymer loop brushes (PLBs).[17] Since the polymer brushes are formed by PSC templates, σ, ε, ε', and *h* can be controlled. Note that the DP of the two polymers allows for achieving similar chain segment blob density profiles along the brush direction in the respective PLBs and STPBs.[30] The molecular weight of both polymers are lower than PCL entanglement molecular weight (M_c ~ 15 kDa) in order to study the loop-induced entanglement effect.[18, 19]

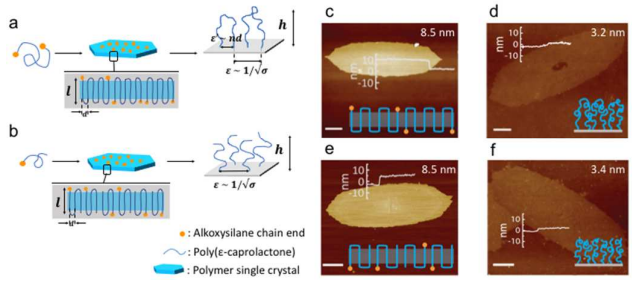

Figure 1. PSC-templated grafting-to method for the preparation of polymer brushes. (a) PLBs; (b) STPBs. (c) & (e) are AFM images of PSCs from $(H_5C_2O)_3Si$-PCL_{56}-$Si(OC_2H_5)_3$ and PCL_{28}-$Si(OC_2H_5)_3$, respectively. (d) & (f) are AFM images of PLBs (d) and STPBs (f). The numbers at the top right corners are the measured brush thickness, and the cartoons at the bottom right corner illustrate the proposed chain conformation (PLB or STPB). Scale bars: 2 μm. (c) and (d) are adapted from Figure 5 in ref. 17.

Figure 1c shows the AFM height image of PSC of the telechelic $(H_5C_2O)_3Si$-PCL_{56}-$Si(OC_2H_5)_3$ grown at 5 °C. Cross-sectional height analysis shows the PSC has a thickness of ~ 8.5 nm. Calculation based on the PCL unit cell structure[31] and the DP suggests that the polymer chains fold 5 times in the crystal (Supporting Information), therefore the two chain ends are located on the same side of the PSC. After washing and re-annealing, PCL PLBs were obtained as shown in Figure 1d with a dry thickness of 3.2 nm. The grafting density of the polymer loop can be calculated as 0.39 chains/nm^2, corresponding to 0.78 tethering points/nm^2. For comparison. STPBs were prepared using PCL_{28}-$Si(OC_2H_5)_3$. Figures 1e, f show the AFM images of PSC of PCL_{28}-$Si(OC_2H_5)_3$ before and after immobilization/washing. The lamellar thickness of the as-prepared PSC is also ~ 8.5 nm, indicating twice-folding. The obtained STPBs exhibit a dry thickness of ~ 3.4 nm, corresponding to a grafting density of 0.81 chains/nm^2 or tethering points/nm^2. The nearly identical grafting density, brush height and chemical structure of these two systems allow us to investigate the brush architectural effect on the mechanical properties of brush-bearing surfaces.

The polymer brushes were firstly studied using AFM-SMFS by bringing a polymer-functionalized AFM cantilever ('hook") to the brush-bearing surface.[32-34] Pyramid-shaped AFM probes were chemically functionalized using PCL_{333}-OH, and the successful attachment of one polymer chain on the tip was confirmed by measuring the adhesion between functionalized AFM probe and freshly cleaved mica surface in toluene following a reported method (Figure S3).[35] Both the PLBs and STPBs samples were then subject to AFM-SMFS measurements in toluene under identical experimental conditions. Immediately following the physical contact between the probe and brush-bearing surfaces, steric repulsion induced by the deformation of the grafted polymer chains resulted significant bending of the cantilever as seen in Figure S4. For both STPBs and PLBs, identical vertical contact position could be identified at D ~ 12 nm based on the algorithm described in the experimental section, confirming that the STPBs and PLBs synthesized herein had similar thickness not only in air, but also in good solvent. On the other hand, larger repulsive force was recorded when PLBs-grafted surface was examined compared with STPBs, which was expected.[12-16]

The retracting portion of the F-D curves were then studied in detail to understand the adhesion behaviour of these polymer brushes. As described in the experimental section, two sets of measurements with different surface dwelling times (0 s or 10 s) were performed on both samples. Out of the approximately 1000 force distance (F-D) curves for each sample tested, when no surface dwelling was applied, 25.2 ± 2.7% (mean ± 95% CI) curves exhibit adhesion characteristics for PLB samples, and 24.2 ± 2.9% for STPB samples. Among them, only nonequilibrium stretching-rupture events are presented (Figures 2a-c), confirming the segmental physical interaction between polymer chain and brushes.[36] The mean adhesion force measured in both STPBs and PLBs samples is small (172 ± 16 pN and 164 ± 24 pN, respectively), as shown in the histogram of Figures 2d-e. Interestingly, for PLB samples, about 0.96 ± 0.67% of the adhesion curves show significantly greater maximum force (Figure 2c), ~ 1.51 ± 0.06 nN, (p < 0.0001 via student's t-test compared with the average 164 ± 24 pN), close to the reported Si-C chemical bond rupture force.[37-39] This suggests that although the molecular weight of the PLB is lower than M_c, the unique loop conformation can form molecular level Velcro-like entanglement with the grafted PCL chain on the AFM probe[14, 40-42] (see later discussion).

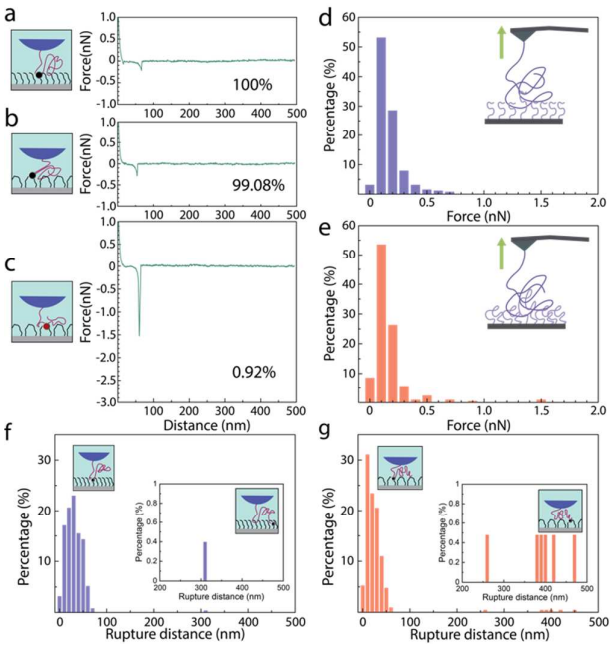

Figure 2. AFM-SMFS measurements with 0s surface dwelling. (a-c) Representative F-D curves on STPBs (a), and PLBs (b, c). (d-e) Histogram of adhesion force on STPBs (d) and PLBs (e). (f-g) Histogram of adhesion rupture distance on PCL STPBs (f) and PLBs (g).

The histogram of rupture distance (tip-surface distance) are also plotted in Figures 2f, g. Considering the contour length of polymers used herein (49 nm for $(H_5C_2O)_3Si$-PCL_{56}-$Si(OC_2H_5)_3$, 24.5 nm for PCL_{28}-$Si(OC_2H_5)_3$, and 333 nm for PCL_{333}-OH),[43] the

interaction between polymer chain and polymer brushes almost exclusively took place at segments close to the AFM probe surface (at rupture distance < 80 nm). This can be explained that when the probe was pushed into polymer brush layers, the segments close to tethering point on AFM tip surface of the grafted PCL chain would more likely to interlock with the brushes, while the free tail was either pushed away or embedded inside the coil.

Since sufficient relaxation of polymer chains are required for the development of entanglement, a 10 s surface dwelling before retraction was introduced. Indeed, the dwelling process significantly affected the adhesion behavior: 1) with surface dwelling, the probability of STPBs and PLBs showing adhesion with AFM probe increased from 24.2 ± 2.9% and 25.2 ± 2.7%, to 34.6 ± 2.5% and 57.1 ± 4.1%, respectively (p < 0.0001 via chi-squared test); 2) for the F-D curves that exhibited adhesion, with 10 s dwelling, STPB-bearing surface still showed weak rupture force (Figure 3a, d) while in the PLB case, the adhesion force was strengthened compared with the non-dwelling case (Figure 2e vs. 3e), and the frequency of strong adhesion due to Velcro-like entanglement drastically increased from 0.96 ± 0.67% to 11.2 ± 0.8% (p < 0.0001 via chi-squared test, Figures 3b, c, e). The distribution of adhesion force was significantly broadened (p < 0.0001 via F-test, Figure 3e); 3) The surface dwelling also greatly increased the probability of long-distance rupture (rupture distance > 100 nm) for PLBs (2.87 ± 1.16% to 9.58 ± 1.66%, p = 0.003) but not for STPBs (0.40 ± 0.40% to 1.12 ± 0.50%, p = 0.32), and the probability increased from 0.5% to 4.5% in STPBs, while in PLBs this number was further raised to 13.1%. These changes can be explained by the increased entanglement between the brush and the AFM probe-bound polymer due to chain relaxation in the dwelling period.[44]

Figure 3h quantitatively compares the different adhesion behavior between these two brush systems in the dwelling-retracting experiments. It is clear that most of the STPB rupture events take place at lower rupture distances and smaller rupture forces compared with PLBs, which can be attributed mainly to the different entanglement behavior of STPB and PLB with the approaching PCL chains. Considering the M_c of PCL in melt (~ 15 kDa),[18, 19] entanglement between the grafted PCL on AFM tip with either STPBs or PLBs should be absent, especially with the presence of good solvent which further increases M_c.[45] However, for PLBs, the unique loop configuration provided effective load-bearing sites for entanglement to be developed,[46] and the breaking of such interaction eventually led to strong adhesion and long rupture distance as shown Figure 3h.

To test the system at macroscale, tap-shear experiments were conducted using a sandwich configuration where a PCL film was confined between two glass substrates coated with STPBs or PLBs, as illustrated in Scheme S2.[47] The adhesion strength of each PCL film/glass slides combination was calculated based on the weight required for the two opposing glass slides to be slide apart (Supporting Information). As seen in Figure 4a, by grafting STPBs onto the glass substrates, as-prepared adhesive joint already showed improvement (0.29 MPa) compared with bare glass surfaces (0.11 MPa). Although based on previous discussion, due to the short molar mass of STPBs, strong entanglement between polymer chains from PCL films and STPBs could rarely be formed, the improved chemical affinity should account for the increased adhesion strength. When PLBs were grafted, the adhesion strength increased drastically (1.56 MPa) compared with both bare glass substrate and STPB-functionalized surface. This significant enhancement again is because of the capability of forming strong Velcro-like molecular entanglement between the polymer chains on PCL film and PLBs as evidenced by previous studies using AFM-SMFS. In order to investigate the repeatability of the strong adhesion joint, two consecutive lap-shear experiments were performed after the joint was broken and the glass surfaces were thoroughly cleaned. As seen in Figure 4a, the obtained adhesion strength from these two experiments [PLBs coated (2^{nd}) & PLBs coated (3^{rd})] are similar compared with the pristine sample, suggesting the adhesive interaction formed between PLBs and PCL film is highly repeatable.

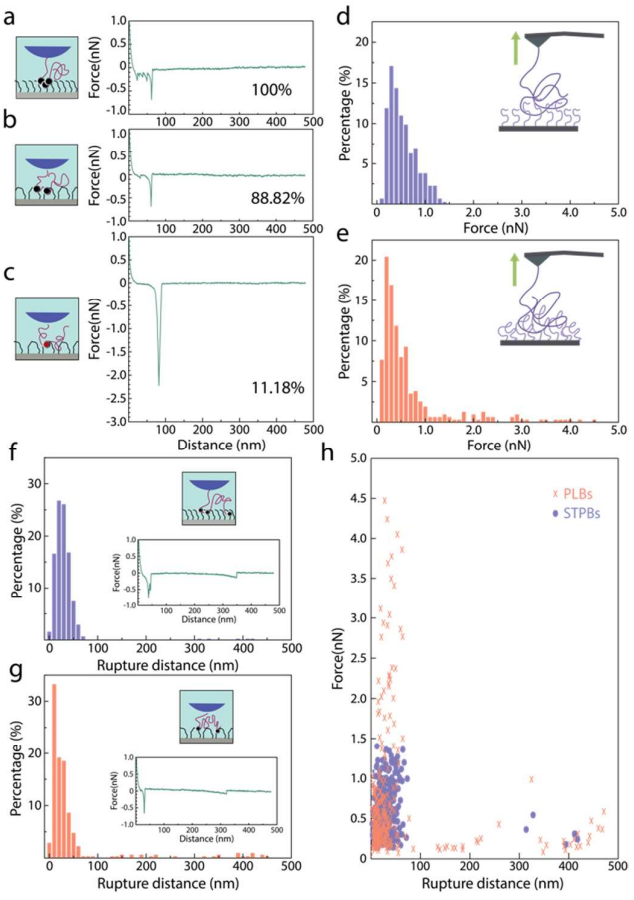

Figure 3. AFM-SMFS measurements with 10s surface dwelling. (a-c) Representative F-D curves on STPBs (a), and PLBs (c,d). (d-e) Histogram of adhesion force on PCL STPBs (d) and PCL PLBs (e). (f-g) Histogram of adhesion rupture distance on PCL STPBs (f) and PLBs (g). The insets of (f) and (g) are representative F-D curves showing adhesion rupture distance much larger than the contour length of polymer brushes. (h) Summary of the adhesion force and corresponding rupture distance obtained from force spectroscopy measurements with 10 s surface dwelling.

The fracture surfaces were imaged using SEM in order to determine the failure mechanism (Figures 4b-i). For adhesion joints of bare glass/PCL film, and STPBs grafted glass/PCL film constructed with 30 min annealing time (Figures 4b-e), the fracture appeared to occur exclusively at the interface between PCL film and glass substrate as the PCL film after the experiments only reside on one surface, indicating an adhesive failure mechanism. However, for PLBs grafted glass/PCL adhesion joints, the fracture surface of the PCL film was in fact quite rough as revealed under SEM (Figure 4f), while the opposing glass surface was partially coated with residue polymers (Figure 4g), suggesting that the materials failed through both cohesive and adhesive mechanism. To further enhance the polymer entanglement at the interface, the PCL film/PLB-coated glass slides were annealed at 80 °C overnight before being cooled to RT for the adhesion test. SEM characterizations of the fractured surfaces displayed in Figures 4h, i reveal rough surfaces of PCL film residual on both slides after the adhesion joint breaks, which suggests a cohesive failure of the bulk PCL film. The measured strength at breaking in Figure 4a shows a significant enhancement (2.83 MPa) compared with adhesion joint prepared at 80 °C for 30 min (1.56 MPa). Note that cohesive failure implies that the measured stress should be smaller than the adhesion strength between PLB-grafted glass substrate and PCL film. This clearly demonstrates that with prolonged contact between PCL chains on film surface with grafted PLBs, the interfacial adhesion can be greatly strengthened due to more "Velcro"-like physical entanglements being developed. Furthermore, compared with literature reported supramolecular recognition-based molecular Velcro adhesive device,[4, 5] the adhesion strength measured here is significantly higher (1.12 MPa vs. 2.83 MPa), which again highlights the improved properties of the "Velcro"-like interactions constructed in this study.

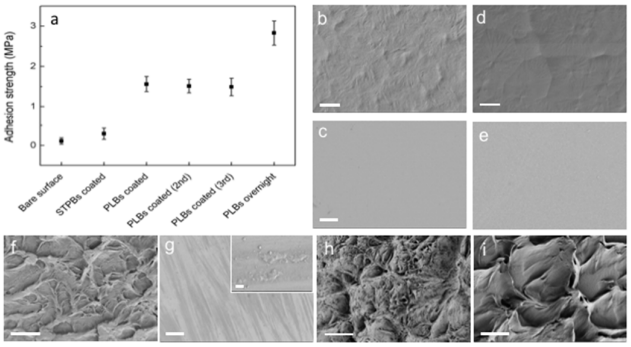

Figure 4. Macroscale adhesion test of molecular Velcro adhesion. (a) Summary of the adhesion strength measured from lap-shear experiments for each glass slides/PCL film combination. (b-i). SEM images of the fracture surfaces of adhesion joint constructed with: (b & c) bare glass and PCL film annealed at 80 °C for 30 min; (d & e) STPBs grafted glass slides and PCL film annealed at 80 °C for 30 min; (f & g) PLBs grafted glass slides and PCL film annealed at 80 °C for 30 min; (h & i) PLBs grafted glass slides and PCL film annealed at 80 °C overnight. The inset of (g) shows the magnified "stripe" area. Scale bar: 1 μm in inset of (g); 10 μm in the rest images.

4. Conclusions

In summary, we have synthesized PCL STPBs and PLBs with nearly identical grafting density, brush heights, and grafting points using the PSC-assisted grafting-to method. The adhesion behaviors of the STPBs and PLBs were investigated at molecular scale using AFM-SMFS and at macroscale using lap-shear experiments. Much greater rupture force and distance were observed when the PCL-functionalized AFM probe was retracted from a PLB-grafting surface compared with a STPB-bearing surface due to Velcro-like chain entanglement constructed between the free dangling polymer chain on AFM probe and PLBs. Lap-shear experiments confirmed that due to the formation of molecular entanglement between PLBs and polymer chains at the interface of PCL film and glass slides, the measured adhesion (2.83 MPa) is significantly stronger than the adhesion joints constructed using STPB-grafted or bare glass slides. While adhesive failure mechanism was confirmed for the breaking of the latter two, cohesve failure was observed in the adhesion joint prepared with PLB-grafted glass slides and PCL film. Our results demonstrated that by using PLBs as the surface functionalization materials, large scale adhesive interfaces based on Velcro-like chain entanglement can be efficiently fabricated.

Conflicts of interest

There are no conflicts to declare.

Acknowledgements

This work was supported by the National Science Foundation Grant CHE 1709119 and DMR 1709136.

Notes and references

1. J. Keckes, I. Burgert, K. Fruhmann, M. Muller, K. Kolln, M. Hamilton, M. Burghammer, S. V. Roth, S. Stanzl-Tschegg and P. Fratzl, *Nat. Mater.*, 2003, **2**, 810-814.
2. Y. B. Tzur, K. L. Wilson and Y. Gruenbaum, *Nat. Rev. Mol. Cell Biol.*, 2006, **7**, 782-788.
3. B. Heras, M. Totsika, K. M. Peters, J. J. Paxman, C. L. Gee, R. J. Jarrott, M. A. Perugini, A. E. Whitten and M. A. Schembri, *Proc. Natl. Acad. Sci. U.S.A.*, 2014, **111**, 457-462.
4. Y. Ahn, Y. Jang, N. Selvapalam, G. Yun and K. Kim, *Angew. Chem. Int. Ed.*, 2013, **52**, 3140-3144.
5. J. Guo, C. Yuan, M. Guo, L. Wang and F. Yan, *Chem. Sci.*, 2014, **5**, 3261-3266.
6. K. Kendall, *Molecular Adhesion and Its Applications the Stiky Universe*, Kluwer Academic, New York, 2001.
7. J. Alonzo, Z. Huang, M. Liu, J. W. Mays, R. G. Toomey, M. D. Dadmun and S. M. Kilbey, II, *Macromolecules*, 2006, **39**, 8434-8439.
8. Z. Huang, J. Alonzo, M. Liu, H. Ji, F. Yin, G. D. Smith, J. W. Mays, S. M. Kilbey, II and M. D. Dadmun, *Macromolecules*, 2008, **41**, 1745-1752.

9. D. Patton, W. Knoll and R. C. Advincula, *Macromol. Chem. Phys.*, 2011, **212**, 485-497.
10. L. Li, B. Yan, L. Zhang, Y. Tian and H. Zeng, *Chem. Commun.*, 2015, **51**, 15780-15783.
11. Y. Han, J. Ma, Y. Hu, J. Jin and W. Jiang, *Langmuir*, 2018.
12. F. Yin, D. Bedrov, G. D. Smith and S. M. Kilbey, II, *J. Chem. Phys.*, 2007, **127**.
13. J.-H. Seo, Y. Tsutsumi, A. Kobari, M. Shimojo, T. Hanawa and N. Yui, *Soft Matter*, 2015, **11**, 936-942.
14. A. Takano, I. Kamaya, Y. Takahashi and Y. Matsushita, *Macromolecules*, 2005, **38**, 9718-9723.
15. G. Morgese, L. Trachsel, M. Romio, M. Divandari, S. N. Ramakrishna and E. M. Benetti, *Angew. Chem. Int. Ed.*, 2016, **55**, 15583-15588.
16. M. Divandari, G. Morgese, L. Trachsel, M. Romio, E. S. Dehghani, J.-G. Rosenboom, C. Paradisi, M. Zenobi-Wong, S. N. Ramakrishna and E. M. Benetti, *Macromolecules*, 2017, **50**, 7760-7769.
17. T. Zhou, H. Qi, L. Han, D. Barbash and C. Y. Li, *Nat. Commun.*, 2016, **7**, 11119.
18. A. Izuka, H. H. Winter and T. Hashimoto, *Macromolecules*, 1992, **25**, 2422-2428.
19. M. Grosvenor and J. Staniforth, *Int. J. Pharm.*, 1996, **135**, 103-109.
20. B. Li, L. Y. Li, B. B. Wang and C. Y. Li, *Nature Nanotech.*, 2009, **4**, 358-362.
21. L. Li, C. Y. Li and C. Y. Ni, *J. Am. Chem. Soc.*, 2006, **128**, 1692-1699.
22. B. Li and C. Y. Li, *J. Am. Chem. Soc.*, 2007, **129**, 12-13.
23. B. B. Wang, B. Li, B. Zhao and C. Y. Li, *J. Am. Chem. Soc.*, 2008, **130**, 11594-11595.
24. B. Li, B. Wang, R. C. M. Ferrier, Jr. and C. Y. Li, *Macromolecules*, 2009, **42**, 9394-9399.
25. S. Mei, H. Qi, T. Zhou and C. Y. Li, *Angew. Chem. Int. Ed.*, 2017, **56**, 1-6.
26. B. Dong, T. Zhou, H. Zhang and C. Y. Li, *ACS Nano*, 2013, **7**, 5192-5198.
27. B. B. Wang, B. Li, B. Dong, B. Zhao and C. Y. Li, *Macromolecules*, 2010, **43**, 9234-9238.
28. B. B. Wang, B. Li, R. C. M. Ferrier and C. Y. Li, *Macromol. Rapid Commun.*, 2010, **31**, 169-175.
29. W. Wang, H. Qi, T. Zhou, S. Mei, L. Han, T. Higuchi, H. Jinnai and C. Y. Li, *Nature communications*, 2016, **7**, 10599-10599.
30. H. S. Gulati, C. K. Hall, R. L. Jones and R. J. Spontak, *J. Chem. Phys.*, 1996, **105**, 7712-7722.
31. H. Hu and D. L. Dorset, *Macromolecules*, 1990, **23**, 4604-4607.
32. H.-J. Butt, B. Cappella and M. Kappl, *Surf. Sci. Rep.*, 2005, **59**, 1-152.
33. D. Wang and T. P. Russell, *Macromolecules*, 2017.
34. Y. Xue, X. Li, H. Li and W. Zhang, *Nat. Commun.*, 2014, **5**, 4348.
35. C. Ortiz and G. Hadziioannou, *Macromolecules*, 1999, **32**, 780-787.
36. B. N. Balzer, M. Gallei, K. Sondergeld, M. Schindler, P. Mueller-Buschbaum, M. Rehahn and T. Hugel, *Macromolecules*, 2013, **46**, 7406-7414.
37. M. Grandbois, M. Beyer, M. Rief, H. Clausen-Schaumann and H. E. Gaub, *Science*, 1999, **283**, 1727-1730.
38. S. W. Schmidt, M. K. Beyer and H. Clausen-Schaumann, *J. Am. Chem. Soc.*, 2008, **130**, 3664-3668.
39. S. W. Schmidt, A. Kersch, M. K. Beyer and H. Clausen-Schaumann, *PCCP*, 2011, **13**, 5994-5999.
40. A. Makke, O. Lame, M. Perez and J.-L. Barrat, *Macromolecules*, 2012, **45**, 8445-8452.
41. S. Deng, Y. Huang, C. Lian, S. Xu, H. Liu and S. Lin, *Polymer*, 2014, **55**, 4776-4785.
42. R. Schnell, M. Stamm and C. Creton, *Macromolecules*, 1999, **32**, 3420-3425.
43. Q. Huang, B. Yang, H. Liu, Y. Zhao and J. Du, *Polym. Chem.*, 2015, **6**.
44. A. Halperin and E. B. Zhulina, *Langmuir*, 2010, **26**, 8933-8940.
45. R. P. Wool, *Macromolecules*, 1993, **26**, 1564-1569.
46. C.-A. Dai, B. J. Dair, K. H. Dai, C. K. Ober, E. J. Kramer, C.-Y. Hui and L. W. Jelinski, *Phys. Rev. Lett.*, 1994, **73**, 2472-2475.
47. L. Ge, S. Sethi, L. Ci, P. M. Ajayan and A. Dhinojwala, *Proc. Natl. Acad. Sci. U.S.A.*, 2007, **104**, 10792-10795.

Table of content

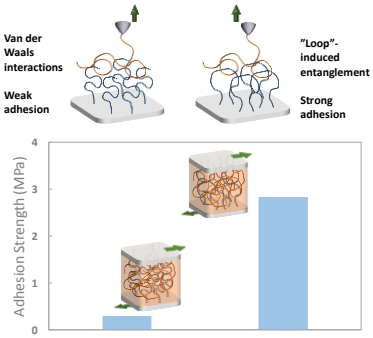

Velcro-mimicking surface based on well-defined polymer loop brushes was fabricated using a polymer single crystal-assisted grafting-to method.